Biochemical characterization of the active heterodimer form of human heparanase (Hpa1) protein expressed in insect cells

Edward McKENZIE*, Kathryn YOUNG*, Margaret HIRCOCK*, James BENNETT*, Maina BHAMAN*, Robert FELIX*, Paul TURNER*, Alasdair STAMPS*, David McMILLAN*, Giles SAVILLE*, Stanley NG*, Sean MASON*, Daniel SNELL*, Darren SCHOFIELD*, Haiping GONG*, Reid TOWNSEND*, John GALLAGHER†, Martin PAGE‡, Raj PAREKH* and Colin STUBBERFIELD*[1]

*Oxford GlycoSciences (OGS), 10 The Quadrant, Abingdon Science Park, Abingdon, Oxon OX14 3YS, U.K., †Department of Medical Oncology, Paterson Institute for Cancer Research, Wilmslow Road, Manchester M20 4BX, U.K., and ‡Oncogene Sciences Inc. Pharmaceuticals, Watlington Road, Oxford OX4 6LT, U.K.

The mammalian endoglycosidase heparanase (Hpa1) is primarily responsible for cleaving heparan sulphate proteoglycans (HSPGs) present on the basement membrane of cells and its potential for remodelling the extracellular matrix (ECM) could be important in embryonic development and tumour metastasis. Elevated expression of this enzyme has been implicated in various pathological processes including tumour cell proliferation, metastasis, inflammation and angiogenesis. The enzyme therefore represents a potential therapeutic target. Hpa1 protein is initially synthesized as an inactive 65 kDa proenzyme that is then believed to be subsequently activated by proteolytic cleavage to generate an active heterodimer of 8 and 50 kDa polypeptides. By analysis of a series of Hpa1 deletion proteins we confirm that the 8 kDa subunit is essential for enzyme activity. We present here for the first time an insect cell expression system used for the generation of large amounts of recombinant protein of high specific activity. Individual subunits were cloned into baculoviral secretory vectors and co-expressed in insect cells. Active secreted heterodimer protein was recovered from the medium and isolated by a one-step heparin–Sepharose chromatography procedure to give protein of > 90 % purity. The recombinant enzyme behaved similarly to the native protein with respect to the size of HS fragments liberated on digestion, substrate cleavage specificity and its preference for acidic pH. A significant amount of activity, however, was also detectable at physiological pH values, as measured both by an *in vitro* assay and by *in vivo* degradation of cell-bound heparan sulphate.

Key words: heparanase, heparanase heterodimer, heparan sulphate.

INTRODUCTION

The extracellular matrix (ECM) is composed of a network of macromolecules that serve to maintain tissue and cellular architecture. In particular, heparan sulphate proteoglycans (HSPGs), consisting of a central protein core covalently linked to several heparan sulphate (HS) polysaccharide chains, make up a significant proportion of the ECM, cell and basement membranes [1,2]. In addition to their role in anchoring cells to matrix fibres and maintaining tissue structure, HSPGs serve at least two additional biological functions. Firstly, the HS chains of these PGs bind to many growth factors and cytokines such as the fibroblast growth factors ('FGFs'), vascular endothelial growth factor ('VEGF') and transforming growth factor ('TGF'). This binding confers resistance on the growth factors to proteolysis and thermal denaturation and provides a reservoir of growth and migration factors that can be mobilized in accordance with physiological demand. Secondly, HSPGs linked to the cell-surface membrane via their core protein act as mandatory co-receptors, facilitating binding of growth factors to their cognate high-affinity signal-transducing receptors (reviewed in [3]). The fact that HS is distributed ubiquitously and evolutionarily conserved demonstrates clearly the importance of this molecule in cell development and function.

Heparanase (Hpa1) cleaves HS side chains, and is thus able to effect degradation of ECM basal membranes with release of

HS-bound growth factors and other molecules involved in tissue repair. Hpa1 activity has been shown in activated leucocytes including T- and B-cells, macrophages, neutrophils and mast cells mediating extravasation and traffic to inflammatory sites [4,5]. In addition, Hpa1 is highly expressed in placental tissue where it is involved in implantation of trophoblast cells [6]. One of the most striking features of Hpa1 is the production of this enzyme in malignant cells and the apparent correlation between elevated levels of Hpa1 activity and metastasis.

The major role played by Hpa1 in malignancy was confirmed by transfection studies with antisense cDNA, which significantly reduced the invasive and metastatic properties of tumour cells [7,8]. A growing body of literature links heparanase expression and the process of tumorigenesis in a wide number of cancers including bladder [9], colon [10], gastric [11], breast [12], oral [13], oesophageal [14], pancreatic [15–17], brain [18] and acute myeloid leukaemia [19]. Collectively, this evidence suggests that Hpa1 plays a fundamental role in sustaining the pathology of malignant diseases and therefore that it may provide a potential target for anti-cancer therapy.

The human *Hpa1* gene, localized on chromosome 4 [20] and encoding a 543-amino-acid protein, has been purified and cloned from platelets [21], placenta [7,22] and fibroblast cell lines [23]. The protein is synthesized as a 65 kDa glycosylated proenzyme that is cleaved subsequently to remove an internal peptide bridge or linker region and form a heterodimer composed of an

N-terminally derived 8 kDa and a C-terminally derived 50 kDa subunit [24]. Although it seems likely that both subunits are essential for activity, this has not been established formally by testing purified components. Primary human fibroblasts have been shown to be capable of binding, internalizing and processing pro-Hpa1 [25]. The cellular localization and secretion of the enzyme is key to its pro-metastatic and pro-angiogenic properties and therefore derivation of enzymically active Hpa1 is likely to be regulated very tightly [26,27]. Activity of the enzyme is controlled tightly by the pH of its environment: at physiological pH values, it is believed that the inactive form of the enzyme is bound to HS [28,29] and that this form only achieves maximum activity under acidic conditions (optimum of pH 5.5–5.8). This pH-dependent aspect may ensure that the structural breakdown of the ECM mediated by heparanase is confined to more acidic conditions, e.g. endosomes and at sites of injury or inflammation. In cancer tissue, a lower pH could be found within the hypoxic areas of a growing tumour [30].

The disclosure of a novel method for the production of abundant quantities of active heparanase protein will be a great aid to biological studies on the enzyme. Availability of the recombinant enzyme would also enable high-throughput screens to identify small-molecule inhibitors. We have addressed this issue by generating recombinant baculovirus using a dual expression vector engineered to produce both heparanase subunits (8 and 50 kDa), tagged for secretion, under control of separate promoters (P10 and polyhedrin). Insect cells infected with recombinant virus secreted Hpa1 heterodimer protein, which could then be recovered to > 90 % purity by a one-step affinity purification using heparin–Sepharose chromatography. Protein obtained by the above procedure was shown to have high levels of enzymic activity as determined by the *in vitro* degradation of ^{35}S-labelled HS. Measurement of heparanase activity confirmed that the optimal enzymic activity of the recombinant enzyme occurs at pH 5.0, which was comparable with that observed using the native enzyme [29,31].

EXPERIMENTAL

Materials

Dithiothreitol, Tris base and FITC were purchased from Sigma (Gillingham, Dorset, U.K.). SDS and Nonidet P-40 were from Fluka (Gillingham, Dorset, U.K.). Peptide N-glycosidase F (N-glycanase) was from Glyko (Novato, CA, U.S.A.). Novex SDS/PAGE, See Blue protein markers and Simply Blue protein stain were all from Invitrogen (Paisley, U.K.). Bovine kidney HS (sodium salt) was from Seikagaku (Falmouth, MA, U.S.A.). TSK-GEL G3000SWxl was from TOSOH Corp. Heparin-Sepharose CL-6B columns and prepacked disposable PD10 columns containing Sephadex G-25 medium were purchased from Amersham Biosciences. Heparin oligosaccharides DP4, DP8 and DP12 were obtained from Iduron (Manchester, U.K.).

Cloning of Hpa1 subunits

Full-length Hpa1 cDNA was PCR amplified from a mammary gland cDNA library (Clontech) using *Pfu* turbo polymerase (Stratagene) and the following cycling conditions: 94 °C for 1 min followed by 30 cycles of 94 °C for 30 s, 60 °C for 30 s and 72 °C for 2 min. PCR products were separated by agarose-gel electrophoresis and a 1.6 kb product was gel purified (Qiaquick; Qiagen) and then cloned into the pZero Blunt vector (Invitrogen). Correct sequence was verified by sequencing with dideoxy dye

terminators (ABI). The small 8 kDa subunit cDNA was then PCR-amplified from this template using the following primers: 8 kDa Forward, 5′-CCC GGG CAG GAC GTC GTG GAC CTG GAC TTC TTC ACC-3′, and 8 kDa Reverse, 5′-GAA TTC TCA TTC CTT CTT GGG ATC GAA AAT TAG GAA-3′. The large subunit was PCR amplified using the following primers: 50 kDa Forward, 5′-CCC GGG AAA AAG TTC AAG AAC AGC ACC TAC TCA AGA-3′, and 50 kDa Reverse, 5′-GAA TTC TCA GAT GCA AGC AGC AAC TTT GGC ATT TCT-3′. Both products were cloned into pZero Blunt, excised by double digestion with *Sma*I/*Eco*RI restriction enzymes (Promega) and ligated into pAcGP67A (Pharmingen) cut with the same enzymes. This cloning strategy generates four extra amino acids on the N-terminus of both subunits.

For construction of the dual expression construct, the 8 kDa subunit cDNA along with flanking GP67 secretory sequence was PCR amplified from the pAcGP67A:8 kDa Hpa1 template using the primers Dual 8 kDa Forward, 5′-AGA TCT ATG CTA CTA GTA AAT CAG TCA CAC CAA GGC-3′, and Dual 8 kDa Reverse, 5′-AGA TCT TCA TTC CTT CTT GGG ATC GAA AAT TAG GAA-3′. The corresponding 50 kDa cDNA with flanking GP67 secretory sequence was PCR amplified from the pAcGP67A:50 kDa Hpa1 template using the primers Dual 50 kDa Forward, 5′-GAA TTC ATG CTA CTA GTA AAT CAG TCA CAC CAA GGC-3′, and Dual 50 kDa Reverse, 5′-GAA TTC TCA GAT GCA AGC AGC AAC TTT GGC ATT TCT-3′. Both PCR products were cloned into pZero Blunt and excised with appropriate enzymes; *Eco*RI for the 50 kDa subunit and *Bgl*II for the 8 kDa subunit. Restriction products were then cloned individually into the appropriately digested pAcUW51 vector (Pharmingen).

Construction of Hpa1 N-terminal deletion proteins

Full-length Hpa1 cDNA prepared as described above was used as the DNA template for all deletion PCR constructs. PCR reactions were carried out using *Pfu* turbo polymerase (Stratagene) and the following cycling conditions: 94 °C for 1 min, followed by 30 cycles of 94 °C for 30 s, 60 °C for 30 s and 72 °C for 2 min. All PCR reactions used the reverse primer 5′-GAA TTC TCA GAT GCA AGC AGC AAC TTT GGC ATT TCT-3′ and the following specific forward primers: 1–35 deletion, 5′-CCC GGG CAG GAC GTC GTG GAC CTG GAC TTC TTC ACC-3′; 1–44 deletion, 5′-CCC GGG ACC CAG GAG CCG CTG CAC CTG GTG AGC CCC-3′; 1–74 deletion, 5′-CCC GGG CTG GGT TCT CCA AAG CTT CGT ACC TTG GCC-3′; 1–85 deletion, 5′-CCC GGG GGC TTG TCT CCT GCG TAC CTG AGG TTT GGT-3′; 1–119 deletion, 5′-CCC GGG TCT CAA GTC AAC CAG GAT ATT TGC AAA TAT-3′; 1–157 deletion, 5′-CCC GGG AAA AAG TTC AAG AAC AGC ACC TAC TCA AGA-3′. PCR products were separated by agarose-gel electrophoresis, and the products were gel purified (Qiaquick) and cloned into the pZero Blunt vector. The correct sequence was verified by sequencing with dideoxy dye terminators (ABI). Products cloned into pZero Blunt were excised by double digestion with *Sma*I/*Eco*RI restriction enzymes (Promega) and ligated into pAcGP67A cut with the same enzymes.

Insect cell expression

Baculovirus transfer vectors containing Hpa1 subunits were co-transfected with Baculogold DNA into Sf9 insect cells grown in SF900II serum-free medium (Gibco BRL) using standard calcium phosphate conditions (Pharmingen). Tni cells cultured

in suspension using ExCell405 serum-free medium (JRH Bioscience) were infected with plaque-pure recombinant viruses at a multiplicity of infection (MOI) of 2 plaque-forming units (pfu) and harvested at 48 h post-infection. Cells were pelleted at 1000 ***g*** for 10 min at 4 °C and crude supernatants containing heparanase kept at 4 °C until purification.

Purification and detection of recombinant heparanase

Routinely, 1.5 litre batches of secreted recombinant heparanase enzyme in ExCell405 medium were passed over a 5-ml heparin–Sepharose Hi-Trap column (Amersham Biosciences) using an FPLC system. Enzyme was loaded at 1 ml/min, column washed in 10 column vol. of wash buffer (150 mM NaCl/25 mM Tris/HCl, pH 7.5) and then eluted with a gradient of 0.15–1.0 M NaCl in 25 mM Tris, pH 7.5, collecting 5-ml fractions. Typically heparanase eluted at 0.67 M NaCl in this system and produced yields of around 1 mg/l. Heparanase was concentrated and buffer exchanged by spinning through a 30-kDa cut-off filter (Vivascience). Proteins were resolved by electrophoresis on SDS/PAGE gels (4–20 %; Invitrogen) followed by staining with Coomassie Brilliant Blue or silver.

Enzyme activity (^{35}S-labelled ECM method)

Measurements of heparanase enzyme activities were carried out as described previously [7]. Essentially, insect cell media containing secreted recombinant enzyme were incubated for 18 h at 37 °C, pH 6.2–6.6, with ^{35}S-labelled HS produced by murine 3T3 cells isolated and characterized as described previously [32]. The incubation medium was centrifuged and the supernatant analysed by gel filtration on a Sepharose CL-6B column (0.9 cm × 30 cm). Fractions were eluted with PBS and their radioactivity measured.

Deglycosylation

Heparanase was denatured by heating to 100 °C for 3 min in deglycosylation buffer (125 mM NaCl/25 mM Tris/HCl/0.1 M dithiothreitol/0.1 % SDS, pH 7.5). Samples were cooled briefly and centrifuged at 10 000 ***g***. SDS was displaced by the addition of Nonidet P-40 to 1 %, after which 10 m-units of N-glycanase was added and samples incubated at 37 °C. N-glycosylation sites were predicted using the NetNGlyc 1.0 prediction (http://www.cbs.dtu.dk/services/NetNGlyc/).

Western blotting

Rabbit polyclonal antibodies were generated by Abcam (Cambridge, U.K.) against a peptide contained within the 8 kDa subunit (KTDFLIFDPKKE, amino acids 98–109) and also within the 50 kDa subunit (LKMVDDQTLPPLMEK, amino acids 501–515). Proteins were separated by SDS/PAGE on a 4–20 % Tris-glycine Novex® gel using Novex® Tris-glycine buffers and transferred to a PVDF membrane using the Novex® transfer system (Invitrogen). MagicMark™ Western standards (0.5 μg) were also loaded on to the gel. The PVDF membrane was subsequently blocked [10 % milk powder in 25 mM Tris/150 mM NaCl, pH 7.4 (TBS), and 0.1 % Tween 20], and then cut into strips. The PVDF strips were incubated with the polyclonal antibody against the 8 kDa subunit (0.33 μg/ml), that against the 50 kDa subunit (1 μg/ml) or both in 5 % BSA in TBS/0.1 % Tween 20 for 24 h at 4 °C. Three other membrane strips were also incubated with the antibodies and 10 μg of the relevant peptide

to show the specificity of the antibody. Following washing with TBS/0.1 % Tween 20, the membrane was incubated with donkey anti-rabbit horseradish peroxidase-conjugated secondary antibody (Amersham Biosciences) for 1 h at room temperature. The membrane was washed again and re-assembled before ECL (Amersham Biosciences) treatment to detect the specific Hpa1 subunits and the MagicMark™ Western Standards on ECL-Hyperfilm.

Human platelet protein extract

Blood was collected from healthy human donors into syringes containing 0.11 M sodium citrate to give a final concentration of 11 mM citrate. Warmed acid/citrate/dextrose (25 g/l sodium citrate/20 g/l glucose/15 g/l citric acid) was then added to 10 % (v/v). The blood was centrifuged at 240 ***g*** for 15 min and the upper platelet-rich plasma layer was removed and placed into a fresh tube. Prostacyclin (800 nM) was added to the platelet-rich plasma, which was then centrifuged at 640 ***g*** for 15 min to pellet the platelets. The platelet-poor plasma was poured off and the pellet was re-suspended in 10 ml of modified Tyrode's solution (137 mM NaCl/11.9 mM NaHCO$_3$/0.4 mM NaH$_2$PO$_4$/2.7 mM KCl/1.1 mM MgCl$_2$/5.6 mM glucose, pH 7.4) at 37 °C. The platelet count was then adjusted to 2×10^8 ml^{-1}. An equal volume of lysis buffer [300 mM NaCl/50 mM Tris, pH 7.2/2 % (v/v) Triton X-100, plus protease inhibitor cocktail (Roche)] was added to the platelet suspension and the lysate was mixed gently and left on ice for 10 min prior to freezing for storage.

FITC labelling of HS

HS was labelled with FITC as described in [22]. Briefly, 5 mg of HS and 5 mg of FITC were dissolved in 1 ml of 0.1 M sodium carbonate buffer (pH 9.5) and incubated at 4 °C for 20 h in the dark with constant rotation. FITC-labelled HS (FITC-HS) was separated from unreacted FITC using a PD-10 desalting column (Amersham Biosciences) equilibrated and eluted with heparanase assay buffer (100 mM sodium acetate/5 mM CaCl$_2$, pH 5.5).

FITC-HS heparanase assay

FITC-HS (1 μg) was digested routinely with recombinant Hpa1 (1 ng) in a 200 μl reaction volume with heparanase assay buffer. Reactions were incubated at 37 °C for an appropriate period and stopped by heating at 100 °C for 5 min. Cold assay buffer (200 μl) was subsequently added and the mixture was centrifuged at 10 000 ***g*** for 5 min to remove insoluble material. The reactions were then analysed using a TSK-GEL G3000SWxl run at 1 ml/min in 50 mM Tris/150 mM NaCl, pH 7.5. Fluorescent reaction products were detected using a W474 fluorescence detector (Waters) and activity determined by measuring the decrease in high-molecular-mass HS species.

Immunocytochemistry

HT29 colon adenocarcinoma cells were plated out at a cell density of 5×10^4/chamber in eight-chamber slides using normal growth medium [McCoy's F-10 medium supplemented with 2 mM glutamine, penicillin/streptomycin and 10 % (v/v) foetal bovine serum], and then incubated overnight at 37 °C in 5 % CO$_2$. Cells were washed twice in PBS before incubation with growth medium without serum containing 0, 100, 500 or 2500 ng/ml Hpa1 heterodimer protein. The slides were incubated at 37 °C in 5 %

CO_2 for 4 and 24 h. Those cells incubated for 24 h had 10 % fetal bovine serum added to the culture medium at 4 h. After incubation with the enzyme, cells were washed twice in PBS before being fixed in 4 % formaldehyde for 10 min at room temperature. Cells were washed in PBS and incubated in permeabilizing buffer (0.1 % Triton X-100/1 % saponin/5 % BSA in PBS, pH 7.4) for 20 min at room temperature. The slides were then incubated at 4 °C overnight with 20 μg/ml F58-10E4 clone anti-HS mono-clonal antibody (10E4; Seikagaku) and 2 μg/ml proprietary monoclonal antibody [Oxford GlycoSciences (UK), Abingdon, Oxon, U.K.] directed against Hpa1 (conjugated with AlexaFluor-488 using the Zenon™ labelling kit; Molecular Probes, Leiden, The Netherlands). All antibodies were made up in permeabilizing buffer. Following a further washing step, the slides were incubated with a Texas Red-labelled secondary antibody directed against mouse IgM (10E4 isotype; Jackson ImmunoResearch Laboratories, West Grove, PA, U.S.A.). Finally, the slides were washed, counterstained with 100 ng/ml 4′,6′-diamidino-2-phenylindole hydrochloride (DAPI), washed and mounted.

Images were captured using a Leica Q550FW workstation, digital camera and fluorescence microscope using the × 40 oil-immersion objective lens. For each experiment, several images were captured per condition per colour channel using identical microscope settings. Multi-colour RGB images were then reconstructed using Corel Photopaint 8. Image analysis involved analysing a 40 000 μm^2 area within colonies of HT29 cells ($\approx$ 10 cell nuclei) and using the histogram function to assess the colour intensity in each colour channel. Three colonies were analysed per condition. Data are shown as mean pixel intensity (for the relevant colour channel) $\pm$ S.E.M.

pH profile

The optimum pH for FITC-HS cleavage by heparanase was conducted using three buffers covering a broad pH range: 100 mM sodium acetate, pH 3.5–6.0; 50 mM Bis-Tris, pH 6.0–7.5; 50 mM Tris, pH 7.0–8.5. All buffers were supplemented additionally with 5 mM $CaCl_2$. Reactions were carried out under standard conditions with FITC-HS (1 μg) substrate and incubated for 2 h at 37 °C. Analysis was conducted as described for the FITC-HS heparanase assay.

Heparanase activity in platelet extracts

Heparanase activity was measured in human platelet extracts using the FITC-HS assay system. Platelet cell-extract protein (10 μg) was incubated with 1 μg of FITC-HS for 20 h at 37 °C. The reactions were stopped and analysis was conducted as described for the FITC-HS heparanase assay.

Amino acid sequence analysis

Protein subunits were separated by SDS/PAGE (10–20 % Tris-glycine) and semi-dry electroblotted on to sequence-grade PVDF membrane (Fluorotrans). The blot was then stained with sulphorhodamine B to visualize bands. Polypeptide bands were excised from the blot using a razor blade and placed in the reaction cartridge of the sequencer. The polypeptide was then subjected to automated liquid-pulse Edman degradation on an Applied Biosystems Procise 494 instrument according to the manufacturer's instructions.

### Capillary ion-pair reverse-phase HPLC coupled to MS (IP-LC/MS)

IP-LC/MS was performed using a modification of the method described previously [33]. A reversed-phase capillary HPLC column (75 μm × 10 cm) was prepared under 750 p.s.i. (= 5175 kPa) using C_{18} packing material (5 μm). The chromatograph was equipped with a PepMap pre-column (300 μm × 1 mm; Dionex, Camberley, Surrey, U.K.) and the gradients were produced with the following solvents: solvent A, 100 % water/8 mM acetic acid/5 mM dibutylamine, and solvent B, 70 % methanol/8 mM acetic acid/5 mM dibutylamine. Column equilibration was carried out using solvent A and the gradient developed to 60 % with solvent B over 35 min. The column was washed over 10 min with 100 % solvent B and re-equilibrated, by returning to initial conditions within 3 min. Pre-column flow rate was set at 350 nl/min with a linear gradient. The liquid chromatograph was attached to an LCQ-Deca (Thermoquest, Hemel Hempstead, Herts., U.K.) with an interface which was constructed in-house at Oxford GlycoSciences. The assembly consisted of an xyz stage carrying the capillary column, emitter and liquid junction and the tip was centred $\approx$ 3 mm from the inlet. The spray voltage was set at $-$ 2000 V. The column eluant was introduced into the LCQ through 5 μm (inner diameter) × 150 μm (outer diameter) uncoated fused silica capillary (New Objective, Cambridge, MA, U.S.A.). The electrospray ionization source temperature was set at 200 °C, spectra were acquired at 3 s/scan over a mass range of 300–1600 m/z, the tube lens offset was 25 V and ion residency time was set at 400 ms.

RESULTS

Cloning and expression of the active heparanase heterodimer enzyme

Previous studies have shown that Hpa1 exists as a 65 kDa precursor which is cleaved subsequently by an as yet unidentified protease(s) to form a heterodimeric protein consisting of non-covalently associated 8 and 50 kDa subunits [24]. The cellular machinery required to process Hpa1 appears to be active only in mammalian cells, as full-length cDNA expressed in insect cells results in low-specific-activity protein and poor expression levels (results not shown). The presence of heparanase protein and or activity has been detected in a variety of subcellular locations (e.g. lysosomes, endosomes and the plasma membrane) as well as in secreted form [27,34]. Exploiting the fact that the enzyme can be secreted naturally, we cloned the 8 and 50 kDa subunits into baculovirus secretory vectors and generated recombinant viruses expressing the individual subunits. The two subunits were expressed readily and secreted into the media of insect cells co-infected with the recombinant viruses, a process which greatly facilitated later downstream purification (Figure 1). Initially, both individual subunits were amplified by PCR from a mammary gland cDNA library and cloned into separate pAcGP67 secretory vectors. Cloning into pAcGP67 generates four additional amino acids at the N-termini of both subunits, which had no detrimental effect on the enzymic activity.

The ability of each individual subunit of Hpa1 or the heterodimer generated in our system to digest HS was determined by a traditional ^{35}S-labelled HS assay as described previously [7] and more routinely by a non-radioactive FITC-HS degradation assay [22]. Briefly, insect cell media containing individually expressed 8 or 50 kDa subunits or co-expressed 8/50 kDa protein subunits were incubated with sulphate-labelled material derived from ECM and the digestion products separated by gel filtration on Sepharose CL-6B columns. Neither the 8 nor the 50 kDa subunit
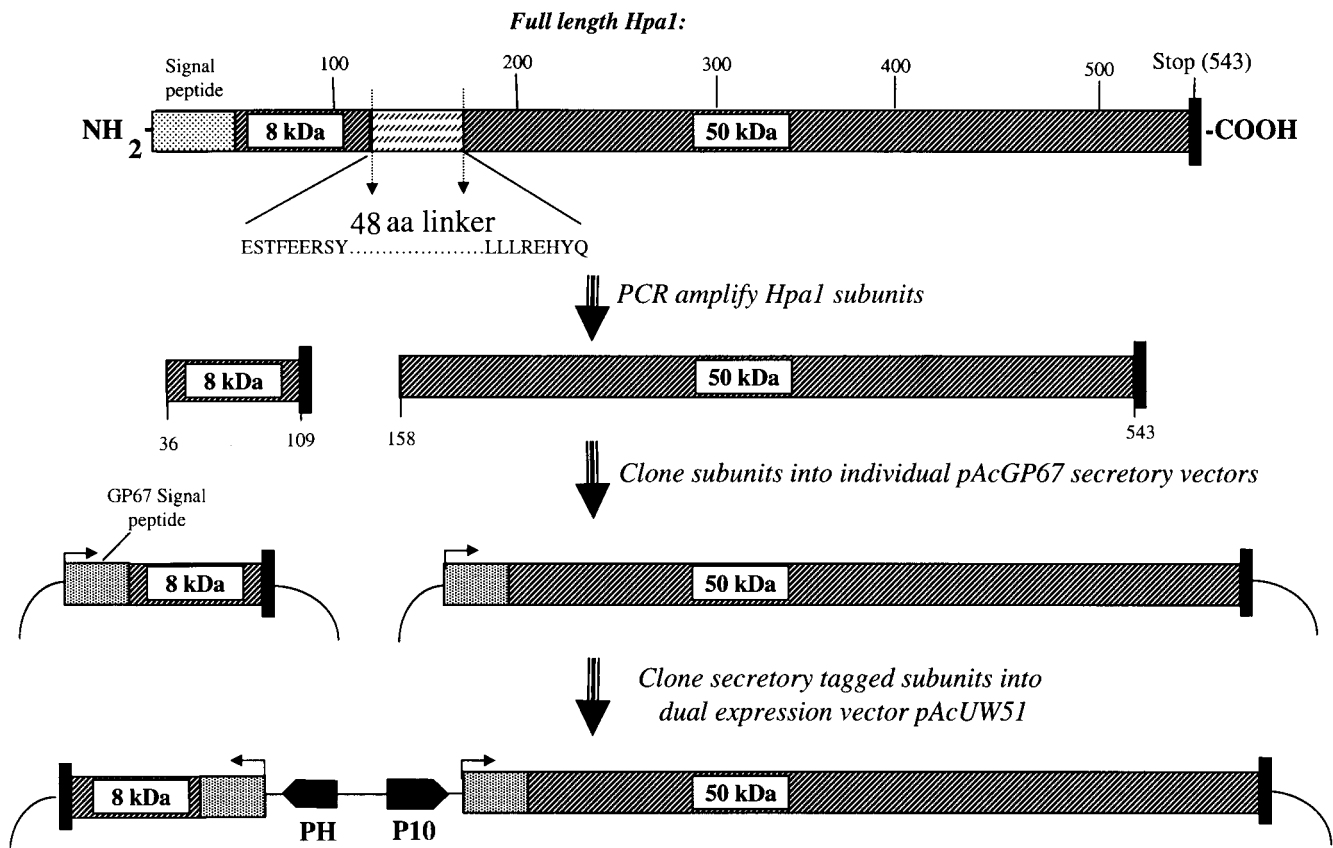
Figure 1   Cloning strategy for the expression of active recombinant Hpa1 heterodimer protein

DNA fragments representing the 8 kDa (amino acids 36–109) and 50 kDa (amino acids 158–543) subunits were PCR-amplified from a full-length clone cDNA. Individual subunit DNAs were first subcloned into the pAcGP67 secretory vector. This construct was then used as a template from which the subunit and corresponding flanking secretory sequence could be PCR-amplified. Finally, tagged subunits were subcloned into the dual expression vector pAcUW51.

on their own was able to digest the HS substrate (Figure 2). In contrast, addition of the 8/50 kDa heterodimer protein medium resulted in a size shift towards low-molecular-mass eluted fragments, indicating a high level of enzymic activity. It is worth noting that attempts at reconstituting the enzyme activity by combining crude supernatant material containing the individually expressed subunits failed to produce active protein (results not shown). This suggested that the subunits needed to intimately fold together within a cellular environment to produce active protein. We have also confirmed Hpa1 heterodimer formation in solution by immunoprecipitation of recombinant Hpa1 with an antibody directed towards the large subunit. SDS/PAGE analysis of the products showed that both subunits were indeed present (results not shown). Western-blotting data (Figure 2B) confirmed expression of the various Hpa1 subunit combinations used in the activity assays.

## Affinity purification of recombinant Hpa1

In order to simplify the expression procedure and to facilitate simultaneous folding of the heterodimer, individual secretory-tagged sequences were cloned into the dual expression vector pAcUW51. Recombinant baculovirus generated using the dual expression vector was plaque purified and a high-titre virus stock generated. Titration of the number of infective viral particles to Tni insect cells, i.e. MOI, was performed with insect cells maintained in serum-free medium, at MOI values of 2, 5 and 10 pfu per cell.

Supernatants and cell pellet material were harvested at 0, 24, 48, 72 and 96 h post-infection and monitored for activity. Optimal conditions of both highest enzyme activity with lowest protein breakdown were observed in the supernatant of cells infected with virus at an MOI of 2 pfu for 48 h (results not shown).

Heparanase was affinity-purified (Figure 3) from crude media by loading slowly at 1 ml/min on to an FPLC heparin–Sepharose Hi-Trap column at 4 °C (during which time ≈80% of the enzyme activity was retained on the column), followed by washing and elution with an increasing salt gradient. Under these conditions heparanase generally eluted at 0.67 M NaCl over three main fractions (Figure 3, fractions 24–26). The small (8 kDa) and large (≈50 kDa) subunits were detected by separating the column fractions by SDS/PAGE, followed by silver staining. The large subunit has a predicted molecular mass of around 46 kDa but ran characteristically as a glycosylated protein with a molecular mass of 46–50 kDa. For convenience we refer to this heterogeneous Hpa1 large subunit protein species as the 50 kDa subunit. This one-step affinity-purification method typically yielded protein of greater than 90% purity and with yields of >1 mg/l. Protein generated by such a method was shown to be extremely stable, with loss of 50% activity after storage for 1 year at 4 °C.

N-terminal sequencing of protein subunits

The identities of the heparanase subunits were confirmed by Edman degradation and N-terminal sequencing. Purified Hpa1

(A)

(B)
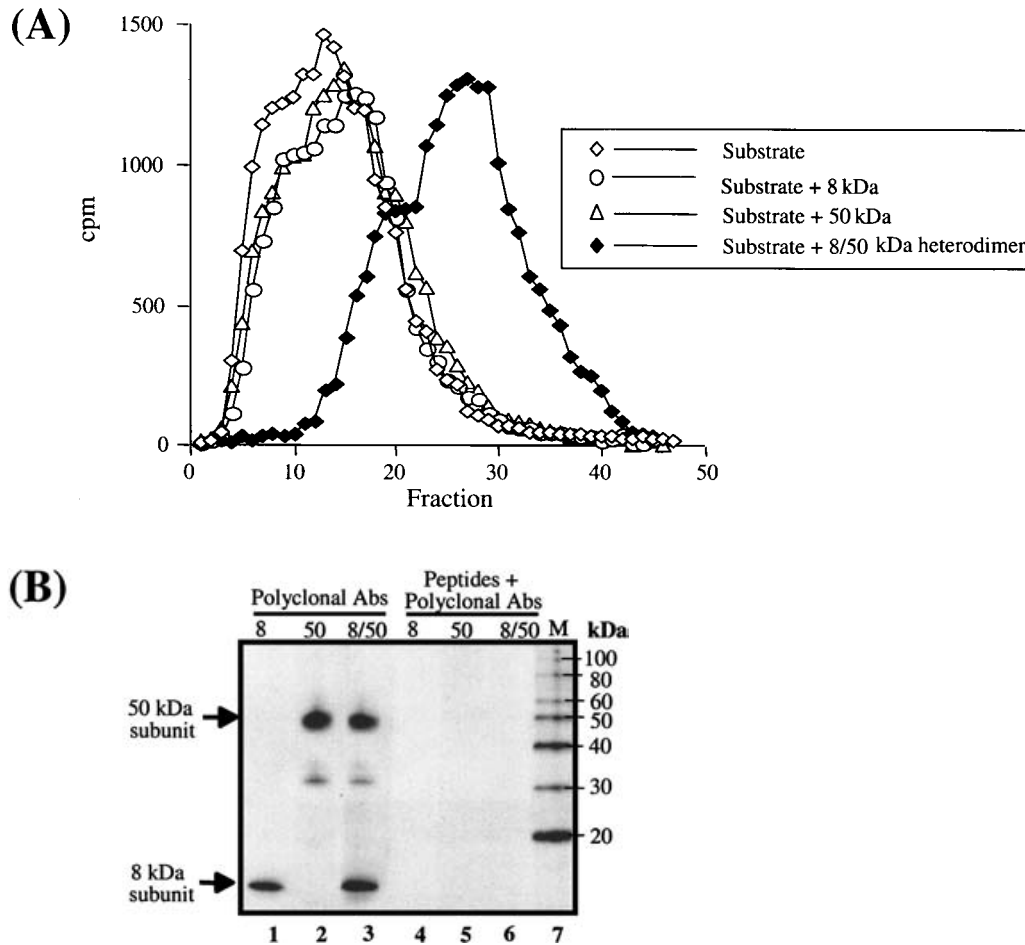
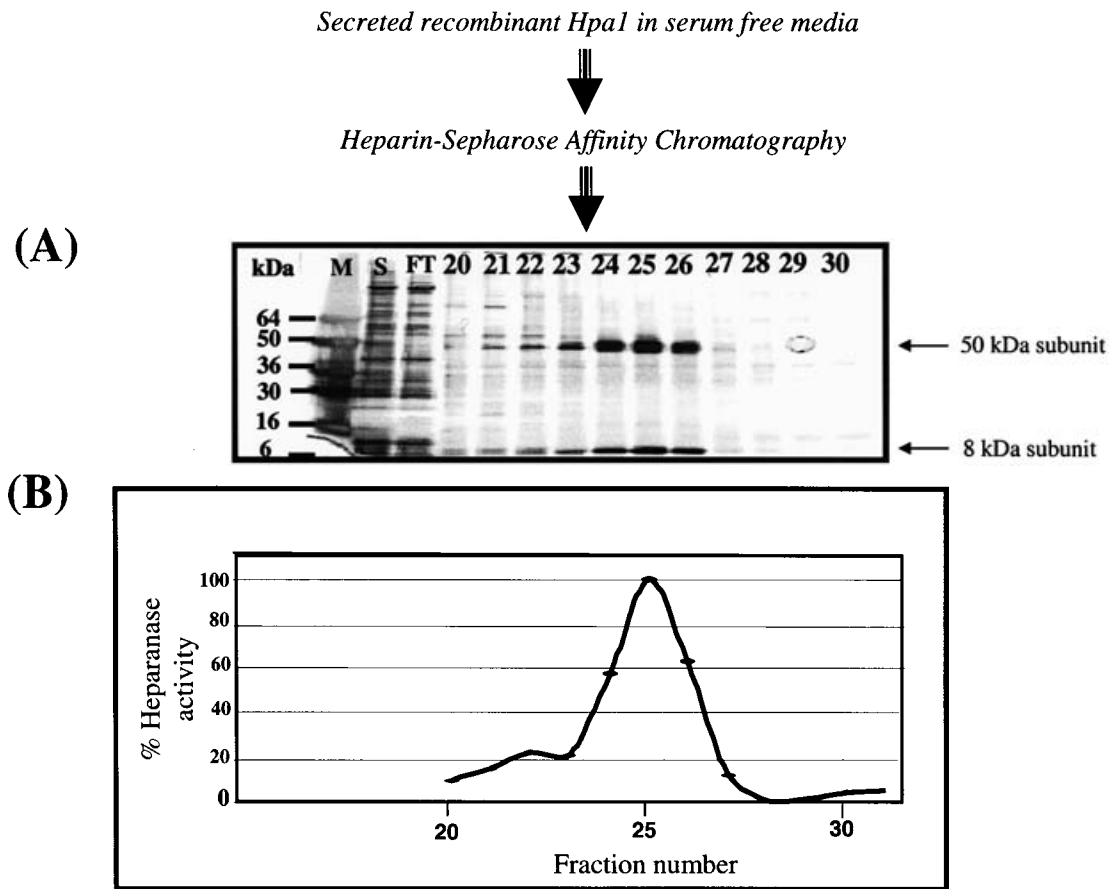**Figure 2   Ability of heparanase subunits to degrade ^{35}S-labelled HS**

(**A**) The culture media were collected from uninfected insect cells, 8-kDa-baculovirus-infected cells, 50-kDa-baculovirus-infected cells and cells infected simultaneously with both 8- and 50-kDa baculovirus (48 h post-infection). Heparanase activity was measured by the degradation of ^{35}S-radiolabelled HS after incubation with the various secreted media fractions. (**B**) The chromatogram shows the gel-filtration profile of the digested HS products as separated on a Sepharose CL-6B column (0.9 cm × 30 cm). Total secreted media protein (30 μg) from each of the secreted media fractions was resolved by SDS/PAGE (4–20 % gels), transferred on to PVDF membrane and blotted against a mixture of rabbit peptide polyclonal antibodies directed towards both 8 and 50 kDa subunits. Peptide inhibition was performed, using an excess of peptide to confirm specificity of the primary antibodies. Detection was carried out using a secondary anti-rabbit antibody conjugated to horseradish peroxidase followed by ECL treatment.

protein subunits were first resolved by SDS/PAGE, electroblotted on to nitrocellulose and subjected to Edman degradation. Ten amino acids were obtained from both the N-terminus of the 8 kDa subunit (sequence NH$_2$-<u>ADPG</u>QDVVDL-COOH; the underlined sequence represents extraneous amino acids produced from the cloning site and the remaining residues cover Hpa1 amino acids Q^{36}–L^{41}. Ten amino acids were also obtained from the N-terminus of the 50 kDa subunit (sequence NH$_2$-<u>ADPG</u>KKFKNS-COOH; the underlining represents extraneous amino acids as above and the remaining six residues cover Hpa1 amino acids K^{158}–S^{163}).

Effect of heparanase N-terminal deletions on enzyme activity

As part of our studies on Hpa1 heterodimer formation, a series of Hpa1 N-terminal truncation constructs was cloned and the truncated proteins expressed in insect cells (Figure 4A). All Hpa1 deletion proteins tested were enzymically inactive when tested individually and only the protein comprising residues 158–543, representing the 50 kDa large subunit showed activity when co-expressed with the 8 kDa subunit (Figure 4B). Interestingly, addition of an extra flanking region at the

N-terminus of the 50 kDa subunit completely destroyed activity. It is unclear yet whether this extraneous sequence at the N-terminal end of the 50 kDa subunit prevents correct heterodimer folding or whether it blocks the enzyme active site. Incubation of an excess of the free linker region polypeptide (corresponding to amino acid region 110–157) with active Hpa1 heterodimer failed to inhibit activity (results not shown), suggesting that it is not the sequence itself that is inhibitory but the fact that it is contiguous with the large subunit. During our expression studies non-specific proteolysis was observed with the singly expressed N-terminal truncation proteins (Figure 4C, lanes 2–6, arrows), suggesting a role for the 8 kDa subunit in correct folding and stabilization of the 50 kDa subunit. Expression of the truncated proteins for an additional 24 h resulted in the complete conversion to the lower form (results not shown). Co-expression of the 8 kDa subunit with each truncation protein (Figure 4D, lanes 2–6) prevented proteolysis, suggesting that the 8 kDa subunit was associating with the truncated Hpa1 forming a heterodimer, thus shielding the complex from degradation. Dual-expressed 50/8 kDa protein heterodimer (Figure 3), shown for comparison (Figures 4C and 4D, lanes 7), was particularly resistant to proteolytic degradation.

Secreted recombinant Hpa1 in serum free media

⇓

Heparin-Sepharose Affinity Chromatography

⇓

(A)

(B)

Figure 3   Method of purifying secreted heparanase protein from insect cell media

Media from cells infected with dual-expressed heparanase 8/50 kDa baculovirus was harvested 48 h post-infection and affinity purified by passing over a heparin–Sepharose Hi-Trap column. The column was washed with Tris-buffered solution and heparanase eluted by salt-gradient elution (0.15–1 M NaCl). Aliqouts from the eluted fractions were resolved by SDS/PAGE (4–20 % gels) and silver stained (**A**). Stained gel shows presence of Hpa1 species in starting material (S), depletion in the post-affinity flowthrough (FT) and elution of enriched heparanase 8/50 kDa species over three main fractions (fractions 24–26). Markers (M) are See Blue. Fractions were also tested for heparanase activity by the standard FITC-HS assay (**B**) and results are represented as a percentage of the maximum activity obtained (activity was calculated as the peak area reduction of the starting undigested HS peak on the HPLC gel-filtration trace). Fractions 24–26 contain the highest observable activity.

Recombinant enzyme has maximum activity at acidic pH

To confirm that our enzyme has a similar activity profile as reported for the native enzyme, standard FITC-HS assays were set up using a range of pH conditions (Figure 5). Three buffering conditions (sodium acetate, Bis-Tris and Tris) were used to ensure good buffering capacity over the pH range 3.5–8.5. Activity was represented by the peak area reduction (mean of triplicate assay points) of the starting undigested HS peak on the HPLC gel-filtration trace. Maximum activity was observed at pH 5.0, which is in accordance with published data. A significant amount of activity ($\approx$ 20 % of maximum) was also observed at pH 7.0.

## Active Hpa1 heterodimer protein degrades cell-surface HS

Increasing amounts of active Hpa1 protein were incubated directly with HT29 colorectal cancer cells in growth medium at pH 7.4 for up to 24 h. Degradation of cell-surface HS was detected using the 10E4 monoclonal antibody and an IgM specific secondary antibody conjugated to the fluorophore Texas Red. This antibody binds to full-length HS chains [35,36]. Hpa1 at 100 ng/ml was shown to significantly degrade cell-surface HS after 4 h (Figure 6A). Higher concentrations of Hpa1 were shown to almost completely remove the 10E4 epitopes from HT29 cells at 4 h,

although by 24 h, some recovery of cell-surface HS had begun (Figure 6b).

The presence of both exogenous and endogenous sources of Hpa1 on the HT29 cell lines was analysed using a proprietary monoclonal antibody developed by Oxford GlycoSciences (UK). This monoclonal antibody has been shown to recognize the large subunit of native Hpa1 in immunoprecipitation experiments of platelet Hpa1 (results not shown). It is clear in the present study that the recombinant Hpa1 heterodimer protein does not enter HT29 cells, in addition to other cancer cell lines examined, such as MDA-MB-435 (results not shown). Taken together, the exclusion of this highly active form of Hpa1 from cells and the concomitant degradation of cell-surface HS provide strong evidence that Hpa1 can act extracellularly at physiological pH values.

N-glycanase treatment of Hpa1

Heparanase is predicted (via the NetNGlyc1.0 prediction programme) to have six potential sites for N-glycosylation, all encoded within the 50 kDa large subunit. To establish the extent of glycosylation on the recombinant Hpa1, the protein was deglycosylated by incubation with N-glycanase (the method is described in [37]). Under the conditions employed a control

(A) <u>Construct</u>
(amino acid position)

(B)

(C)

(D)
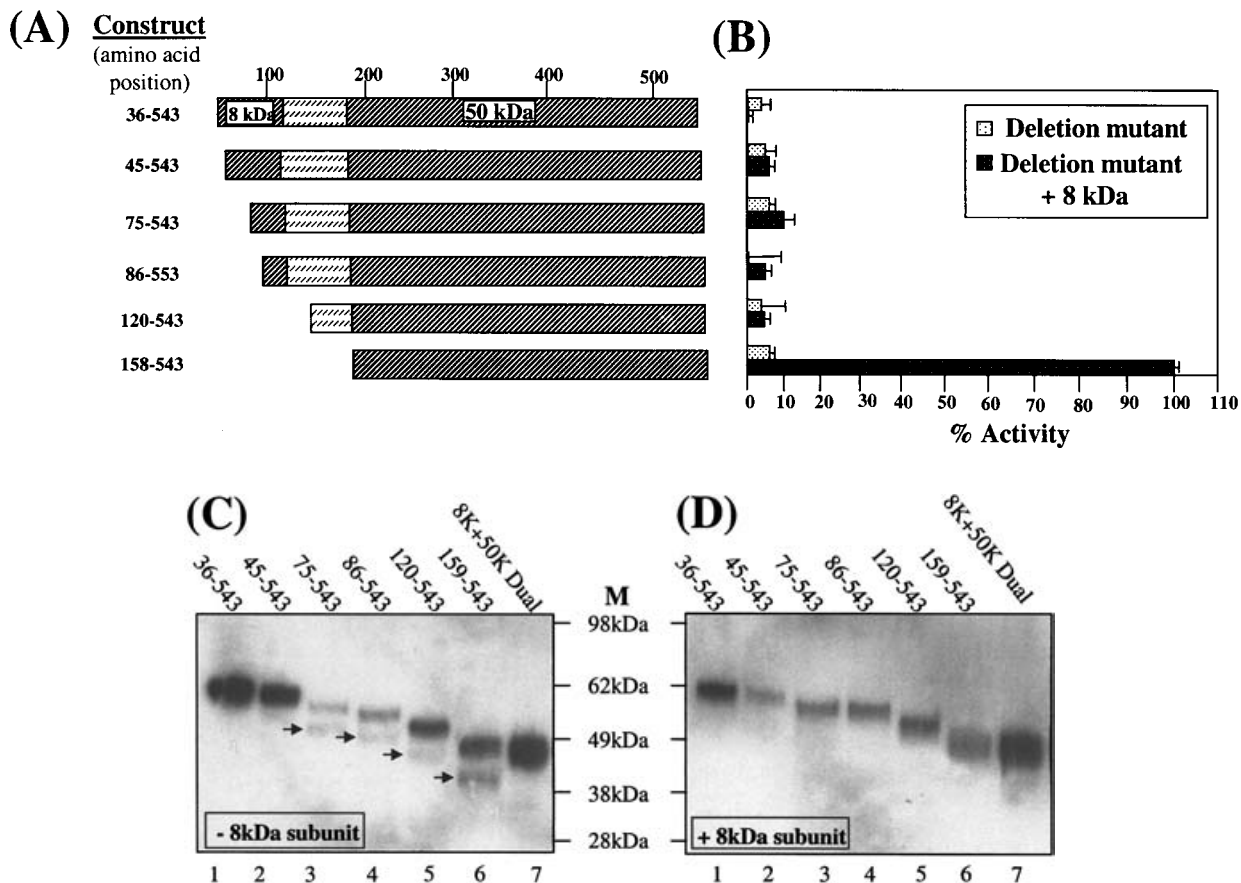
Figure 4   Effect of heparanase N-terminal deletions on enzyme activity

A series of N-terminal Hpa1 deletion constructs were PCR amplified (**A**) and cloned into a baculovirus secretory vector for infection into insect cells. All truncation proteins were secreted into the medium. Enzyme activities were measured from either singly expressed Hpa1 truncation proteins or as a heterodimer complex with the 8 kDa subunit (**B**) using the standard FITC-HPLC assay. Activities are represented as a percentage of the maximum activity achieved by the 8/50 kDa heterodimer complex. Western-blot analysis using an anti-Hpa1 antibody (directed towards the 50 kDa subunit) shows singly expressed protein truncations (**C**) and protein truncations co-expressed with the 8 kDa subunit (arrows indicate Hpa1 breakdown products; **D**). Dual-expressed Hpa1 8/50 kDa complex is shown in lane 7 of each blot for comparison.
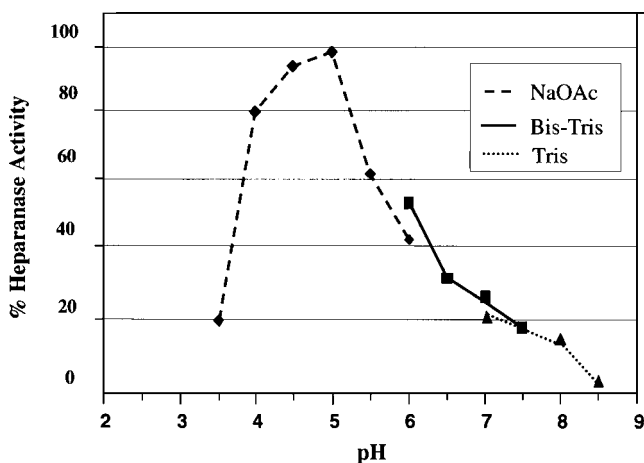

Figure 5   pH dependence of heparanase activity

The FITC-HS heparanase assay was conducted using buffers covering the pH range 3.5–8.5. To ensure good buffering capacity three buffers were used: sodium acetate (NaOAc) for pH 3.5–6.0, Bis-Tris for pH 6.0–7.5 and Tris for pH 7–8.5. Activity was calculated as the peak area reduction of the starting undigested HS peak on the HPLC gel filtration (mean of triplicate assays) and is represented as a percentage of the maximum activity obtained.

protein, RNaseB, was shown to be deglycosylated completely (results not shown). Treatment with N-glycanase for 18 h resulted in incomplete deglycosylation (Figure 7A; lanes 1 and 2 show untreated and treated samples respectively). The sample at this point was visibly cloudy and so was centrifuged to fully evaluate the amount of soluble material remaining. In Figure 7(A), lane 3 (soluble fraction) shows only the presence of the small subunit whereas lane 4 (pellet fraction) shows that the vast majority of protein has precipitated from solution. A limited digestion of recombinant Hpa1 with N-glycanase for 5 h discriminated seven discrete-molecular-mass species (Figure 7A, see the right-hand panel), representing the 'naked' deglycosylated form and six additional glycoforms, exactly as predicted (Figure 7B). Interestingly, both the extension of incubation to 36 h and the use of larger amounts of N-glycanase were unable to completely deglycosylate the Hpa1 large subunit, suggesting the presence of alternative post-translational additions (results not shown). Attempts to maintain the solubility of the Hpa1 large subunit by N-glycanase digestion in the presence of high concentrations of detergent (1 % SDS for the denaturation reaction and 10 % Nonidet P-40 for the digest) were unsuccessful (results not shown). Glycosylation of Hpa1 appeared therefore to be essential for solubility of the large subunit and is consistent with our finding that the 50 kDa subunit expressed in *Escherichia coli* was found in insoluble inclusion bodies.

(A)

HT29 colonies at 4hrs

Control

100ng/mL

500ng/mL

(B)
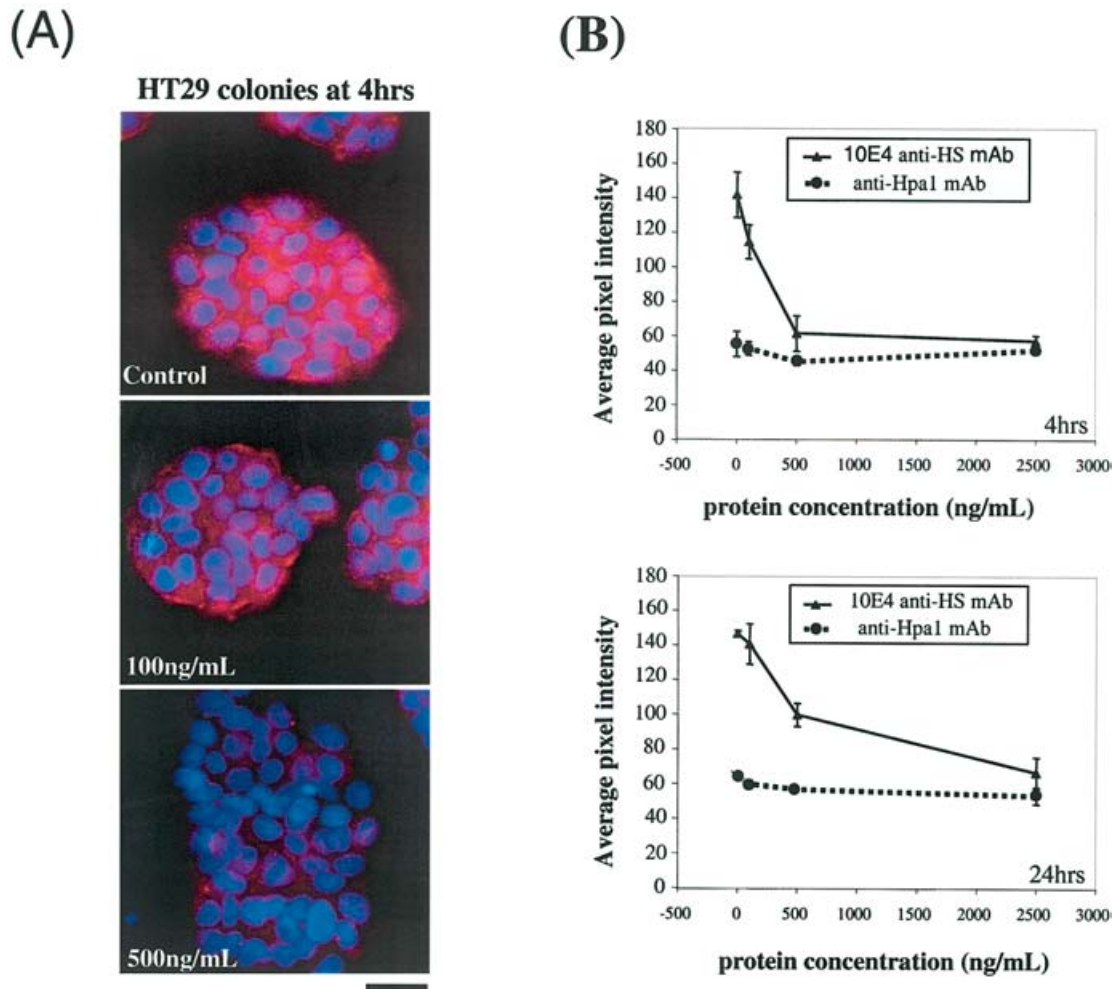
Figure 6   Exogenous addition of active Hpa1 protein to HT29 cells degrades cell-surface HS

Increasing concentrations of active Hpa1 protein were applied directly to a culture of HT29 cells seeded on to chamber slides and incubated for 4 and 24 h. Cells were fixed, permeabilized and stained simultaneously with anti-Hpa1 monoclonal antibody (AlexaFluor-488-conjugated) and with an anti-HS antibody (10E4) overnight at 4 °C. Anti-HS staining was detected with an anti-IgM Texas Red-conjugated secondary antibody and the nuclei counterstained with DAPI. Fluorescent images (**A**) show levels of HS staining (red) at different concentrations of Hpa1 protein at the 4 h time point; cell nuclei are stained blue and no Hpa1 is visible. Image quantification analysis (**B**) was performed on groups of ≈ 10 HT29 cells (see the Experimental section for details). Graphs show a representative analysis (mean pixel intensity ± S.E.M.).

Comparison of HS degradation profiles produced by recombinant and native heparanase enzyme

Whereas our recombinant enzyme degraded HS, it was important to confirm that the processing activity was comparable with that obtained with Hpa1 derived from native sources. To this end the HS degradation profile produced by recombinant enzyme was compared with that obtained from human platelet extracts. An excess of protein in each case was incubated with FITC-HS, the reaction was allowed to run to completion and samples were analysed by gel-filtration HPLC. Data (Figure 8) showed that the profile of the recombinant enzyme was completely indistinguishable from that of the native enzyme, confirming the fidelity of the recombinant expression system.

### MS analysis of recombinant heparanase cleavage specificity

The substrate specificity of the heparanase enzyme for sulphated oligosaccharides has already been examined carefully [38,39]. From these and other studies [40–43] a consensus cleavage region for Hpa1 has been proposed (Figure 9D). Whereas the HS degradation assay (Figures 2 and 8) suggested that the recombinant and native enzymes liberated similar-sized oligosaccharides, it did not provide information on the sulphation of the sugar residues around the cleavage site. In order to address this, a mixture of heparin tetrasaccharides (from a bacterial lyase digest) was digested with recombinant Hpa1 and the substrates and products were analysed using IP-LC/MS. Figure 9(A) shows the chromatographic profile of the tetrasaccharide fraction with the two major peaks corresponding to the penta- and hexa-sulphated species (eluting at 25.7–26.2 and 29 min respectively). After digestion with Hpa1, a new major species was observed at 22.3 min (Figure 9B, *). The mass spectrum of this fraction (Figure 9C, showing major signals at m/z values of 751.9, 672.1, 592.5 and 880.7) corresponds to the molecular masses of species from the tri-sulphated trisaccharide, which is consistent with cleavage at the glucuronic acid residue (GlcUA; Figure 9D). Only a minor proportion of the tetrasaccharide was cleaved by Hpa1 and both longer incubations times and addition of greater concentrations of enzyme failed to increase this amount (results

(A)

(B)
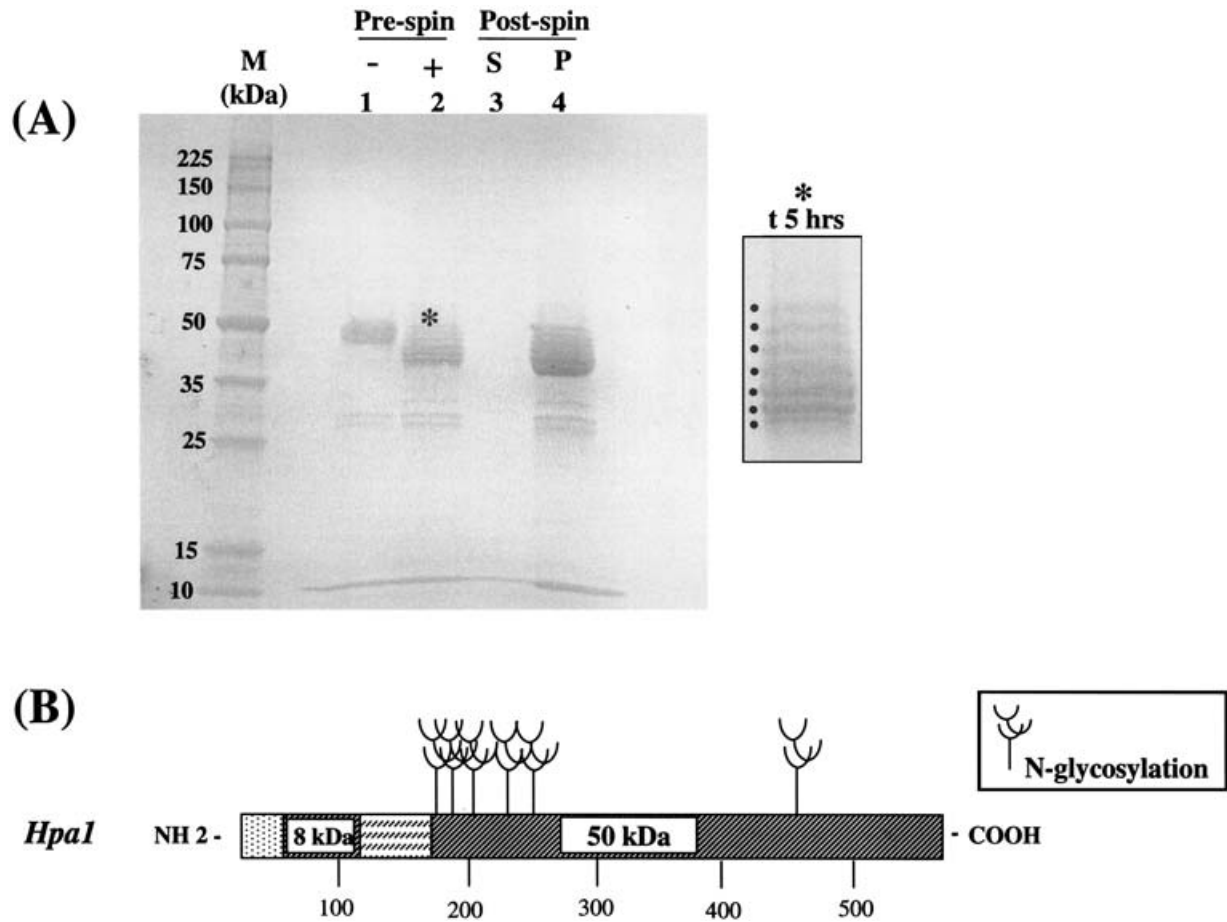
Figure 7   N-glycanase treatment of recombinant heparanase protein

Recombinant Hpa1 was digested with an excess of N-glycanase for 5 h (the right-hand panel, marked *, shows a limited digest producing seven discrete species) and 18 h (**A**) at 37 °C. Proteins were resolved by SDS/PAGE (4–20 % gels) and stained with Simply Blue stain. Samples are molecular-mass markers (M), lane 1 (no glycanase control), lane 2 (18 h digestion, total digest), lane 3 (18 h digest, post-centrifugation; soluble material remaining) and lane 4 (18 h digest, post-centrifugation; pellet-insoluble material). (**B**) Putative N-linked glycosylation sites on full-length pro-Hpa1 based on prediction software (NetNGlyc1.0). Approximate amino acid positions are shown.
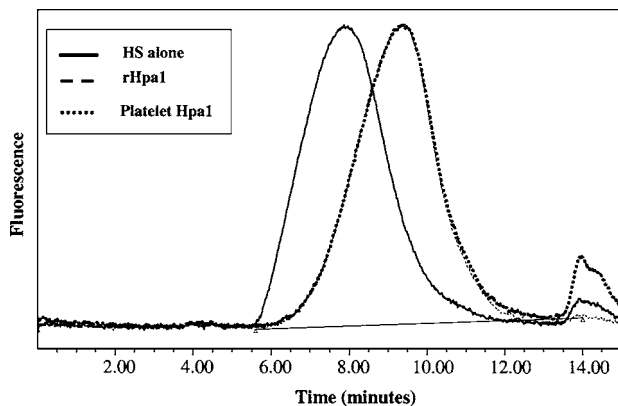

Figure 8   Comparison of HS degradation activity profiles between recombinant and native heparanase enzymes

FITC-HS was digested to completion with either recombinant Hpa1 (rHpa1; 1 ng) or human platelet extract (10 μg) by digestion for 20 h in standard pH 5.5 assay buffer at 37 °C. Samples were resolved individually by gel-filtration HPLC and traces overlaid to allow comparisons of the digestion profiles.

not shown). The low rate of conversion was not unexpected as the majority of the internal uronate residues in heparin are iduronate or iduronate 2-*O*-sulphate and their glycosidic linkages are resistant to Hpa1.

DISCUSSION

This paper is the first to report a method for the production of recombinant active heparanase enzyme which by-passes the need for proteolytic cleavage of the pro-enzyme. Fairbanks and colleagues [24] have suggested previously that the human enzyme is actually a two-chain enzyme consisting of tightly associated, but non-covalently linked, 8 and 50 kDa subunits. Crucially, however, these authors failed to demonstrate any form of reconstitution experiment showing evidence of an obligate heterodimer. Our work provides compelling evidence that the active enzyme is indeed a heterodimer and describes a rapid and efficient method to generate high levels of enzymically active heparanase enzyme in an insect cell expression system. In addition, it explains why early attempts by us and others [7,20] to express only the mature 50 kDa subunit failed to yield active enzyme.
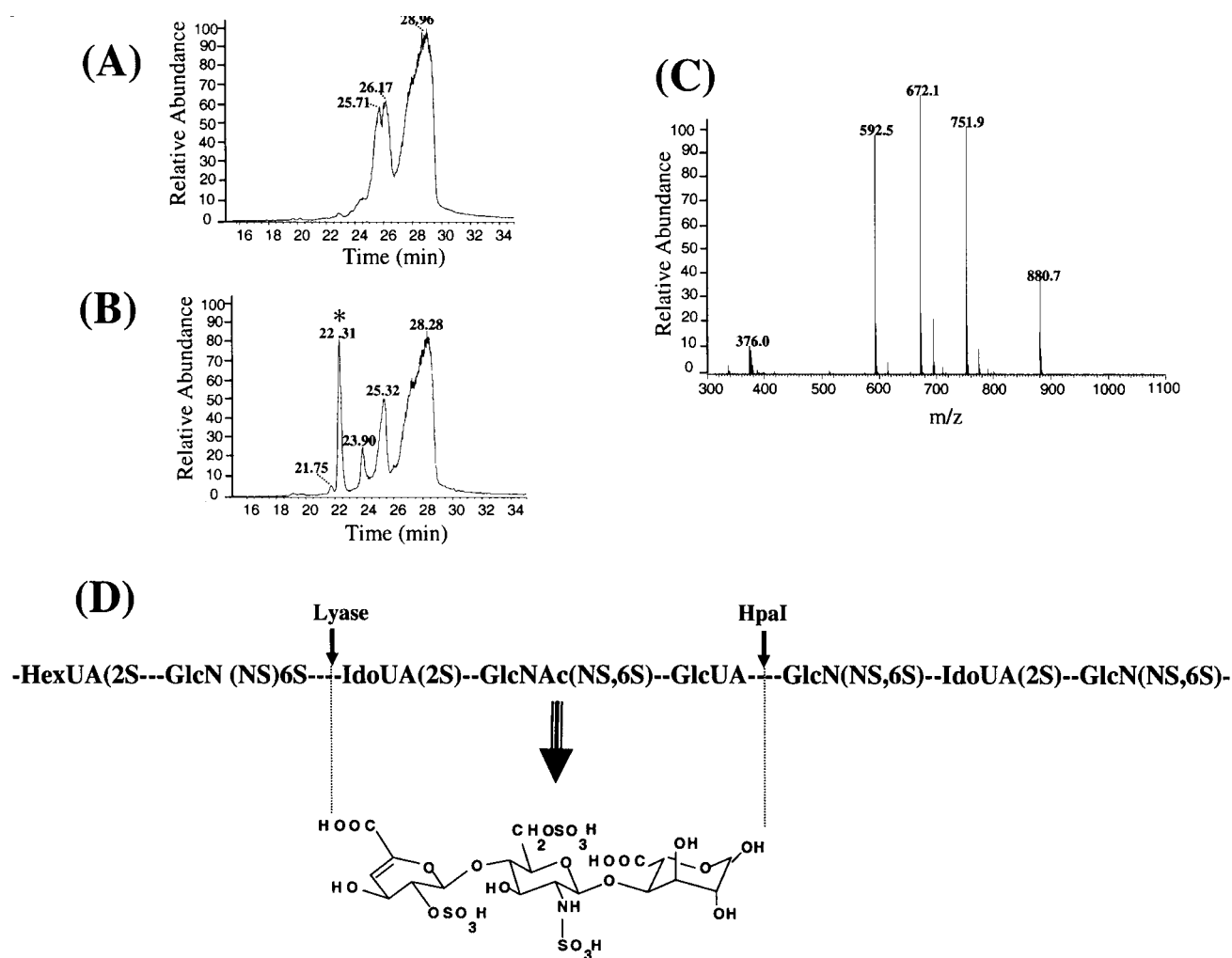
Figure 9　Analysis by IP-LC/MS of heparin tetrasaccharide products after Hpa1-mediated digestion

Heparin tetrasaccharide (10 μg; Iduron DP4) was digested with 1 μg of recombinant Hpa1 in standard assay buffer for 16 h at 37 °C and products analysed by IP-LC/MS (**B**). An aliquot (1 ng in a volume of 4 μl) was diluted in solvent A and injected into the capillary LC/MS as described in the Experimental section. A control with no enzyme (**A**) is shown for comparison. The new fragment generated at a retention time of 22.31 min (**B**; *) was analysed further by MS (**C**) and produced ions of m/z 751.8, 672.1, 592.5 and 880.7. Consensus cleavage sites on HS by Hpa1 and bacterial lyase are indicated and the fragments assigned as DP3 with three sulphates (**D**). GlcUA, glucuronic acid; HexUA, hexuronic acid; IdoUA, iduronic acid.

Analogies can be drawn between the mechanism of activation of pro-heparanase and pro-caspase, where excision and loss of a peptide bridge spanning N-terminal and C-terminal polypeptides gives rise to the active two-chain heterodimer caspase. The mechanism of proteolytic processing of the inactive or latent pro-heparanase, however, is still unclear, as is the fate of its excised linker peptide. The processing enzymes are believed to be released into the culture medium of tumour cells and may normally reside on the cell surface [7,25]. The linker peptide may directly block the enzyme active site or physically distort the interaction between subunits. The actions of a protease(s) on this hydrophilic and presumably cell-surface-exposed linker region would then relieve this constraint and allow access of HS substrate to the catalytic site. Our work suggests that complete removal of the linker is probably required for activity and that cleavage at a single site (amino acid position 109) is insufficient. It remains to be determined, however, whether single cleavage at the other site (amino acid position 158), leaving a 49 amino acid overhang at the C-terminal end of the 8 kDa subunit, is sufficient to permit enzyme activation. The active-site residues [44] and putative heparan-binding domains are all encoded within the large subunit so the

role of the 8 kDa subunit is unclear. Work is currently underway in this laboratory to define, by mutagenesis, the minimum domain within the 8 kDa subunit essential for interaction within the heterodimer. A true understanding of the transition between pro-enzyme and active heterodimeric enzyme will only come from detailed crystal structure studies, which are ongoing.

Our finding that heparanase retains activity at physiological pH values *in vitro* is consistent with other published work [29,45]. However, the finding that the enzyme can degrade cell-bound HS when applied exogenously to cells contradicts the general view that the protein is only active under inflamed or anoxic situations at acidic pHs. No evidence was found that the externally applied active form of the protein was taken into intracellular organelles with significantly lower pH values, such as endosomes or lysosomes. Such intracellular organelles are thought to be the site of action of endogenous Hpa1 in some cell lines [34,46,47] where the enzyme is thought to play an important role in the degradation and recycling of HSPGs. In our studies, active Hpa1 was excluded from the cells even at very high concentrations of protein. An extracellular mode of action for Hpa1 has been recently suggested to be important in

tumour invasion and metastases [27] and so the present study provides further credence to the idea that cell-surface-anchored or secreted forms of Hpa1 heterodimer expressed by invasive cancer cells may well have biological activity at physiological pH. It is also conceivable, for example, that circulating Hpa1 heterodimer protein may possess sufficient intrinsic enzymic activity to have some role in remodelling the HS architecture of endothelial cells lining blood vessels.

The recombinant Hpa1 described here degraded HS to fragment sizes similar to those produced by the native enzyme and cleaved a heparin tetrasaccharide to a defined DP3 species in a pattern consistent with known cleavage-specificity sites. Additional studies with more highly purified heparan-derived oligosaccharides will be required to define precisely the influence of groups remote to the heparanase-cleavage site. Overall, the results are in agreement with previous studies showing that heparanase recognizes a small, highly sulphated region of heparan chains. As well as determining enzymic activity *in vitro*, we have also studied the recombinant enzyme in a number of biological cell-based assays such as motility and angiogenesis. In these cases, exogenous addition of enzyme was shown both to increase dramatically the rate of motility of PC3 cells through an invasion chamber and to increase the tubule length and degree of branching of endothelial cells in angiogenesis assays (P. Turner, E. McKenzie, M. Hircock, J. Bennett, M. Bhaman, R. Felix and C. Stubberfield, unpublished work). Our studies have indicated that there are six N-linked glycosylation sites on Hpa1 and that the presence of N-glycans is important in maintaining the solubility of the 50 kDa subunit. The glycosylation patterns of proteins produced via the insect cell route is different from those produced in mammalian systems and so more work must be carried out to assess fully whether subtle differences in the repertoire of glycosylation on Hpa1 has a functional consequence for the activity of the protein.

Tissue-remodelling enzymes, including the matrix metalloproteinases and heparanase, have received renewed attention as putative targets for anti-cancer therapies since they contribute to both metastasis and angiogenesis. Several inhibitors of matrix metalloproteinases have reached clinical trials, although initial results suggest that this approach may prove too toxic and may even stabilize pre-existing tumour growth (reviewed in [48,49]). Since the matrix metalloproteinases consist of a large family of molecules, it is perhaps not surprising that their inhibition is sometimes associated with deleterious side effects. The heparanase enzyme may prove to be a more specific target for anti-cancer therapy and currently two inhibitors of heparanase, the oligosaccharide PI-88 [50] and the relatively non-specific inhibitor suramin [51], are undergoing clinical trials as anti-tumour agents. Potential drawbacks with these inhibitors are risks of haemorrhage with extended treatment due to the anti-coagulant properties and non-selectivity through unwanted disruption of protein–oligosaccharide interactions. The ability to generate large amounts of active heparanase will not only benefit research into the biology of this important enzyme but also facilitate high-throughput screening strategies to develop more specific and selective inhibitors. It is envisaged that new inhibitory molecules will serve as key tools to evaluate the role of Hpa1 in disease processes and may further prove to be clinically relevant in the treatment of cancer and inflammatory conditions.

REFERENCES

1   Kjellen, L. and Lindahl, U. (1991) Proteoglycans: structures and interactions. Annu. Rev. Biochem. **60**, 443–475

2   Bernfield, M., Gotte, M., Park, P. W., Reizes, O., Fitzgerald, M. L., Lincecum, J. and Zako, M. (1999) Functions of cell surface heparan sulfate proteoglycans. Annu. Rev. Biochem. **68**, 729–777

3   Vlodavsky, I., Bar-Shavit, R., Korner, G. and Fuks, Z. (1993) Extracellular matrix-bound growth factors, enzymes and plasma proteins. In Basement Membranes: Cellular and Molecular Aspects (Rohrback, D. H. and Timpl, R., eds.), pp. 327–343, Academic Press, Orlando, FL

4   Vaday, G. G. and Lider, O. (2000) Extracellular matrix moieties, cytokines, and enzymes: dynamic effects on immune cell behavior and inflammation. J. Leukocyte Biol. **67**, 149–159

5   Schor, H., Vaday, G. G. and Lider, O. (2000) Modulation of leukocyte behavior by an inflamed extracellular matrix. Dev. Immunol. **7**, 227–238

6   Dempsey, L. A., Plummer, T. B., Coombes, S. L. and Platt, J. L. (2000) Heparanase expression in invasive trophoblasts and acute vascular damage. Glycobiology **10**, 467–475

7   Vlodavsky, I., Friedmann, Y., Elkin, M., Aingorn, H., Atzmon, R., Ishai-Michaeli, R., Bitan, M., Pappo, O., Peretz, T., Michal, I., Spector, L. and Pecker, I. (1999) Mammalian heparanase: gene cloning, expression and function in tumor progression and metastasis. Nat. Med. **5**, 793–802

8   Uno, F., Fujiwara, T., Takata, Y., Ohtani, S., Katsuda, K., Takaoka, M., Ohkawa, T., Naomoto, Y., Nakajima, M. and Tanaka, N. (2001) Antisense-mediated suppression of human heparanase gene expression inhibits pleural dissemination of human cancer cells. Cancer Res. **61**, 7855–7860

9   Gohji, K., Okamoto, M., Kitazawa, S., Toyoshima, M., Dong, J., Katsuoka, Y. and Nakajima, M. (2001) Heparanase protein and gene expression in bladder cancer. J. Urol. **166**, 1286–1290

10 Friedmann, Y., Vlodavsky, I., Aingorn, H., Aviv, A., Peretz, T., Pecker, I. and Pappo, O. (2000) Expression of heparanase in normal, dysplastic, and neoplastic human colonic mucosa and stroma. Evidence for its role in colonic tumorigenesis. Am. J. Pathol. **157**, 1167–1175

11 Tang, W., Nakamura, Y., Tsujimoto, M., Sato, M., Wang, X., Kurozumi, K., Nakahara, M., Nakao, K., Nakamura, M., Mori, I. and Kakudo, K. (2002) Heparanase: a key enzyme in invasion and metastasis of gastric carcinoma. Mod. Pathol. **15**, 593–598

12 Maxhimer, J. B., Quiros, R. M., Stewart, R., Dowlatshahi, K., Gattuso, P., Fan, M., Prinz, R. A. and Xu, X. (2002) Heparanase-1 expression is associated with the metastatic potential of breast cancer. Surgery **132**, 326–333

13 Ikuta, M., Podyma, K. A., Maruyama, K., Enomoto, S. and Yanagishita, M. (2001) Expression of heparanase in oral cancer cell lines and oral cancer tissues. Oral Oncol. **37**, 177–184

14 Mikami, S., Ohashi, K., Usui, Y., Nemoto, T., Katsube, K., Yanagishita, M., Nakajima, M., Nakamura, K. and Koike, M. (2001) Loss of syndecan-1 and increased expression of heparanase in invasive esophageal carcinomas. Jpn. J. Cancer Res. **92**, 1062–1073

15 Koliopanos, A., Friess, H., Kleeff, J., Shi, X., Liao, Q., Pecker, I., Vlodavsky, I., Zimmermann, A. and Buchler, M. W. (2001) Heparanase expression in primary and metastatic pancreatic cancer. Cancer Res. **61**, 4655–4659

16 Rohloff, J., Zinke, J., Schoppmeyer, K., Tannapfel, A., Witzigmann, H., Mossner, J., Wittekind, C. and Caca, K. (2002) Heparanase expression is a prognostic indicator for postoperative survival in pancreatic adenocarcinoma. Br. J. Cancer **86**, 1270–1275

17 Kim, A. W., Xu, X., Hollinger, E. F., Gattuso, P., Godellas, C. V. and Prinz, R. A. (2002) Human heparanase-1 gene expression in pancreatic adenocarcinoma. J. Gastrointest. Surg. **6**, 167–172

18 Marchetti, D. and Nicolson, G. L. (2001) Human heparanase: a molecular determinant of brain metastasis. Adv. Enzyme Regul. **41**, 343–359

19 Vlodavsky, I., Goldshmidt, O., Zcharia, E., Atzmon, R., Rangini-Guatta, Z., Elkin, M., Peretz, T. and Friedmann, Y. (2002) Mammalian heparanase: involvement in cancer metastasis, angiogenesis and normal development. Semin. Cancer Biol. **12**, 121–129

20 Dong, J., Kukula, A. K., Toyoshima, M. and Nakajima, M. (2000) Genomic organization and chromosome localization of the newly identified human heparanase gene. Gene **253**, 171–178

21 Hulett, M. D., Freeman, C., Hamdorf, B. J., Baker, R. T., Harris, M. J. and Parish, C. R. (1999) Cloning of mammalian heparanase, an important enzyme in tumor invasion and metastasis. Nat. Med. **5**, 803–809

22 Kussie, P. H., Hulmes, J. D., Ludwig, D. L., Patel, S., Navarro, E. C., Seddon, A. P., Giorgio, N. A. and Bohlen, P. (1999) Cloning and functional expression of a human heparanase gene. Biochem. Biophys. Res. Commun. **261**, 183–187

23 Toyoshima, M. and Nakajima, M. (1999) Human heparanase. Purification, characterization, cloning, and expression. J. Biol. Chem. **274**, 24153–24160

24 Fairbanks, M. B., Mildner, A. M., Leone, J. W., Cavey, G. S., Mathews, W. R., Drong, R. F., Slightom, J. L., Bienkowski, M. J., Smith, C. W., Bannow, C. A. and Heinrikson, R. L. (1999) Processing of the human heparanase precursor and evidence that the active enzyme is a heterodimer. J. Biol. Chem. **274**, 29587–29590

25 Nadav, L., Eldor, A., Yacoby-Zeevi, O., Zamir, E., Pecker, I., Ilan, N., Geiger, B., Vlodavsky, I. and Katz, B. Z. (2002) Activation, processing and trafficking of extracellular heparanase by primary human fibroblasts. J. Cell Sci. **115**, 2179–2187

26 Goldshmidt, O., Zcharia, E., Aingorn, H., Guatta-Rangini, Z., Atzmon, R., Michal, I., Pecker, I., Mitrani, E. and Vlodavsky, I. (2001) Expression pattern and secretion of human and chicken heparanase are determined by their signal peptide sequence. J. Biol. Chem. **276**, 29178–29187

27 Goldshmidt, O., Zcharia, E., Abramovitch, R., Metzger, S., Aingorn, H., Friedmann, Y., Schirrmacher, V., Mitrani, E. and Vlodavsky, I. (2002) Cell surface expression and secretion of heparanase markedly promote tumor angiogenesis and metastasis. Proc. Natl. Acad. Sci. U.S.A. **99**, 10031–10036

28 Gilat, D., Hershkoviz, R., Goldkorn, I., Cahalon, L., Korner, G., Vlodavsky, I. and Lider, O. (1995) Molecular behavior adapts to context: heparanase functions as an extracellular matrix-degrading enzyme or as a T cell adhesion molecule, depending on the local pH. J. Exp. Med. **181**, 1929–1934

29 Ihrcke, N. S., Parker, W., Reissner, K. J. and Platt, J. L. (1998) Regulation of platelet heparanase during inflammation: role of pH and proteinases. J. Cell. Physiol. **175**, 255–267

30 Tannock, I. F. and Rotin, D. (1989) Acid pH in tumours and its potential for therapeutic intervention. Cancer Res. **49**, 4373–4384

31 Freeman, C. and Parish, C. R. (1998) Human platelet heparanase: purification, characterization and catalytic activity. Biochem. J. **330**, 1341–1350

32 Gallagher, J. T. and Walker, A. (1985) Molecular distinctions between heparan sulphate and heparin. Analysis of sulphation patterns indicates that heparan sulphate and heparin are separate families of N-sulphated polysaccharides. Biochem. J. **230**, 665–675

33 Kuberan, B., Lech, M., Zhang, L., Wu, Z. L., Beeler, D. L. and Rosenberg, R. D. (2002) Analysis of heparan sulfate oligosaccharides with ion pair-reverse phase capillary high performance liquid chromatography-microelectrospray ionization time-of-flight mass spectrometry. J. Am. Chem. Soc. **124**, 8707–8718

34 Goldshmidt, O., Nadav, L., Aingorn, H., Irit, C., Feinstein, N., Ilan, N., Zamir, E., Geiger, B., Vlodavsky, I. and Katz, B. Z. (2002) Human heparanase is localized within lysosomes in a stable form. Exp. Cell Res. **281**, 5–62

35 David, G., Bai, X. M., Van der Schueren, B., Cassiman, J. J. and Van den Berghe, H. (1992) Developmental changes in heparan sulfate expression: *in situ* detection with mAbs. J. Cell Biol. **119**, 961–975

36 van Kuppevelt, T. H., Dennissen, M. A., van Venrooij, W. J., Hoet, R. M. and Veerkamp, J. H. (1998) Generation and application of type-specific anti-heparan sulfate antibodies using phage display technology. Further evidence for heparan sulfate heterogeneity in the kidney. J. Biol. Chem. **273**, 12960–12966

37 Tarentino, A. L. and Plummer, Jr, T. H. (1994) Enzymatic deglycosylation of asparagine-linked glycans: purification, properties, and specificity of oligosaccharide-cleaving enzymes from *Flavobacterium meningosepticum*. Methods Enzymol. **230**, 44–57

38 Pikas, D. S., Li, J. P., Vlodavsky, I. and Lindahl, U. (1998) Substrate specificity of heparanases from human hepatoma and platelets. J. Biol. Chem. **273**, 18770–18777

39 Okada, Y., Yamada, S., Toyoshima, M., Dong, J., Nakajima, M. and Sugahara, K. (2002) Structural recognition by recombinant human heparanase that plays critical roles in tumor metastasis. Hierarchical sulphate groups with differential effects and the essential target disulfated trisaccharide sequence J. Biol. Chem. **277**, 42488–42495

40 Yamada, S., Sakamoto, K., Tsuda, H., Yoshida, K., Sugahara, K., Khoo, K. H., Morris, H. R. and Dell, A. (1994) Structural studies on the tri- and tetrasaccharides isolated from porcine intestinal heparin and characterization of heparinase/heparitinases using them as substrates. Glycobiology **4**, 69–78

41 Yamada, S., Yamane, Y., Tsuda, H., Yoshida, K. and Sugahara, K. (1998) A major common trisulfated hexasaccharide core sequence, hexuronic acid(2-sulfate)-glucosamine(N-sulfate)-iduronic acid-N-acetylglucosamine-glucuronic acid-glucosamine(N-sulfate), isolated from the low sulfated irregular region of porcine intestinal heparin. J. Biol. Chem. **273**, 1863–1871

42 Chuang, W. L., Christ, M. D., Peng, J. and Rabenstein, D. L. (2000) An NMR and molecular modeling study of the site-specific binding of histamine by heparin, chemically modified heparin, and heparin-derived oligosaccharides. Biochemistry **39**, 3542–3555

43 Nader, H. B., Porcionatto, M. A., Tersariol, I. L., Pinhal, M. A., Oliveira, F. W., Moraes, C. T. and Dietrich, C. P. (1990) Purification and substrate specificity of heparitinase I and heparitinase II from *Flavobacterium heparinum*. Analyses of the heparin and heparan sulfate degradation products by ^{13}C NMR. J. Biol. Chem. **265**, 16807–16813

44 Hulett, M. D., Hornby, J. R., Ohms, S. J., Zuegg, J., Freeman, C., Gready, J. E. and Parish, C. R. (2000) Identification of active-site residues of the pro-metastatic endoglycosidase heparanase. Biochemistry **39**, 15659–15667

45 Miao, H. Q., Navarro, E., Patel, S., Sargent, D., Koo, H., Wan, H., Plata, A., Zhou, Q., Ludwig, D., Bohlen, P. and Kussie, P. (2002) Cloning, expression, and purification of mouse heparanase. Protein Expr. Purif. **26**, 425–431

46 Tumova, S., Hatch, B. A., Law, D. J. and Bame, K. J. (1999) Basic fibroblast growth factor does not prevent heparan sulphate proteoglycan catabolism in intact cells, but it alters the distribution of the glycosaminoglycan degradation products. Biochem. J. **337**, 471–481

47 Cheng, F., Mani, K., van den Born, J., Ding, K., Belting, M. and Fransson, L. A. (2002) Nitric oxide-dependent processing of heparan sulfate in recycling S-nitrosylated glypican-1 takes place in caveolin-1-containing endosomes. J. Biol. Chem. **277**, 44431–44439

48 Overall, C. M. and Lopez-Otin, C. (2002) Strategies for MMP inhibition in cancer: innovations for the post-trial era. Nat. Rev. Cancer **2**, 657–672

49 Egeblad, M. and Werb, Z. (2002) New functions for the matrix metalloproteinases in cancer progression. Nat. Rev. Cancer **2**, 161–174

50 Iversen, P. O., Sorensen, D. R. and Benestad, H. B. (2002) Inhibitors of angiogenesis selectively reduce the malignant cell load in rodent models of human myeloid leukemias. Leukemia **16**, 376–381

51 Uchio, E. M., Linehan, W. M., Figg, W. D. and Walther, M. M. (2003) A phase I study of intravesical suramin for the treatment of superficial transitional cell carcinoma of the bladder. J. Urol. **169**, 357–360